

Robust Active Force Control of A Quadcopter

Mustakim Omar¹, Musa Mailah^{1,*} and Sherif I. Abdelmaksoud²

¹Faculty of Mechanical Engineering
Universiti Teknologi Malaysia
81310 UTM Johor Bahru
Johor, Malaysia

² Department of Aerospace Engineering
King Fahd University of Petroleum & Minerals
PO Box #526, Dhahran 31261, Eastern Province
Saudi Arabia

ABSTRACT

Outdoor quadrotor helicopter quadcopter operation needs a robust control system in controlling its attitude and altitude to cater for various unmodeled disturbances and uncertainties. Although many control techniques have been tested and applied in quadrotor control systems, the active force control (AFC) scheme has yet to be implemented and investigated. The AFC strategy works via the appropriate manipulation of specific parameters of interest, namely, the estimated mass moment of inertia, measured torque and measured acceleration produced by the system. In this paper, a proportional-integral-derivative (PID) with AFC (PID+AFC) strategy was successfully implemented in altitude (Z-axis) and yaw control of a quadcopter system via simulation. The PID+AFC controller performance was benchmarked with the conventional PID control considering different operation flight paths subject to various forms of disturbances. Simulation results showed that the PID+AFC scheme has significantly improved the altitude control where the steady state error can be reduced up to 70%, particularly with the presence of Z-axis disturbance. The proposed scheme also reacts faster and maintains the quadcopter hovering stability state condition. A slight improvement in yaw control with the application of PID+AFC approach was also observed in comparison to the PID only control.

Keywords: Quadcopter, PID+AFC scheme, robust, altitude and yaw control, disturbances

1.0 INTRODUCTION

Technology innovation has grown significantly, particularly in the field of robotics, due to its great diversity and applicability in different areas; the quadrotor helicopter or quadcopter system is considered one of them. Due to many advantages of the quadrotor features, it has been widely used in applications such as aerial surveillance, aerial photography and video, monitoring traffic pattern analysis, maintenance, search and rescue, meteorological reconnaissance, strategic military task, intelligence and covert operation.

*Corresponding author: musa@fkm.utm.my

Quadcopter system is typically a vertical take-off and landing (VTOL) aircraft [1] consisting of four propellers attached to the main body, either arranged in a '+'-shape or 'x'-shape formation. It is typically a non-linear with a six degree-of-freedom (DOF) system, comprising two fixed pitch clockwise spinning propellers and two counter-clockwise spinning rotors which diagonally oppose each other. Therefore, it is considered underactuated non-linear dynamic system because its control inputs are lower than its DOF. Further, it consists of two subsystems; the translational subsystem (X , Y and altitude Z) and the rotational subsystem (roll ϕ , pitch θ and yaw ψ). The quadcopter most distinguished features are light weight, payload capability, good maneuverability (hovering, VTOL [2]), simplicity in construction and maintenance [3, 4], simple mechanics and relatively small in dimension. These traits have attracted many researchers to further exploit its usefulness and potentials in a variety of ever expanding applications.

Many studies have been carried out for improving the performance, robustness and stability of quadrotor system by concentrating on the novel design and configuration, navigation and flight control systems, control strategies, dynamic stability, trajectory tracking, collision avoidance and others. A number of concepts and breakthroughs have been proposed in the control area. Various linear control strategies have been suggested by researchers such as the classical PID control [5-7], linear-quadratic regulator (LQR) [7] and H_{∞} [8]. Also, non-linear control strategies have been proposed, for instance the backstepping approach [9], sliding mode control [10], model predictive controller [11] and fuzzy [12].

One of the innovative strategies related to the control area is implementing the active force control (AFC) technique because of its effectiveness, robustness and the very fact that the AFC method can be readily and seamlessly integrated with classical, modern and intelligent control. To date, a feedback control strategy based on a PID with AFC scheme has never been tested or investigated on a quadcopter system. Due to its simplicity, high efficiency and robust control approach, it was widely used in many other control system applications such as robotic arms [13-16], vehicle suspension system [17], hard disk drive [18], spacecraft/satellite system [19] and host of others.

In this paper, a mathematical model and control of a quadcopter subjected to external disturbances and unmodeled uncertainties are demonstrated based on *Newton-Euler* method and by utilizing PID with AFC (PID+AFC) strategy for improving the performance and stability of the non-linear system and for increasing the effectiveness and robustness of the proposed control strategy.

2.0 SYSTEM MODELING

In this paper, a mathematical model for a quadrotor aircraft was first derived and adapted based on the works done in [20]. The model consists of two main parts; the first is related to the translational system of equations while the other is on the rotational system of equations. The quadrotor aircraft is a highly non-linear system having multi-input-multi-output (MIMO) configuration, strongly coupled and underactuated system, essentially equipped four actuators [21]. This model is derived, taking into account a number of assumptions to simplify the dynamics of the complex system intended for subsequent simulation. These assumptions are as follows:

- i. The quadrotor structure is rigid and symmetrical with the center of the mass aligned with the center of the body frame of the aircraft.
- ii. The thrust and drag of each motor is proportional to the square of the motor velocity.

- iii. The propellers are considered to be rigid and hence the blade flapping is deemed negligible, i.e., the deformation of the propeller blades due to high velocities and flexible material is ignored.
- iv. The ground effect is neglected.

2.1 Definition and Basic Concepts

It is best to describe the movement and attitude of the quadcopter in two coordinate systems. Figure 1 depicts the basic coordinate system of a quadrotor including the *Euler* angles of roll (ϕ), pitch (θ) and yaw (ψ), a body coordinate frame $\{b\}$, and the global coordinate frame $\{G\}$. This notation is based on the North, East, Down (NED) coordinate system. The position of the quadcopter is given in the global frame while the velocity and angular velocities are defined in the quadrotor body frame.

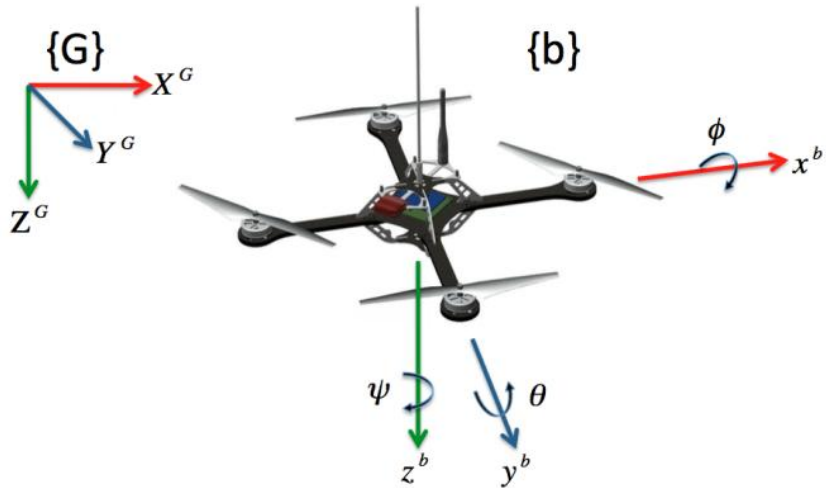


Figure 1: Basic quadcopter structure

There are four basic movements of the quadcopter, which allow the operator to reach the desired altitude, attitude and position as illustrated in Figure 2. The vertical movement, i.e., the *Thrust*, U_1 in [N] is obtained by increasing (or decreasing) all the propeller speeds by the same amount. The roll movement, *Roll*, U_2 in [Nm] corresponds to a rotation of the quadcopter about the x^b axis, it is obtained by increasing (or decreasing) ω_2 and by decreasing (or increasing) ω_4 . The pitch movement, *Pitch*, U_3 in [Nm] corresponds to a rotation of the quadcopter about the y^b axis, it is obtained by increasing (or decreasing) ω_1 and by decreasing (or increasing) ω_3 . The yaw movement, *Yaw*, U_4 in [Nm] corresponds to a rotation of the quadcopter about the z^b axis, it is obtained by increasing (or decreasing) the pair $\omega_1 - \omega_3$ and by decreasing (or increasing) the pair $\omega_2 - \omega_4$.

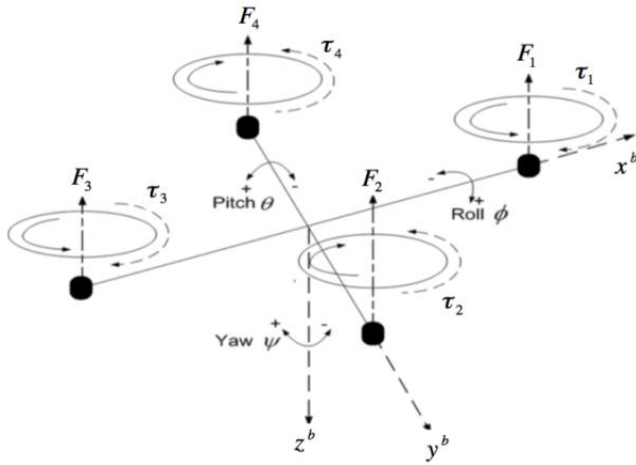


Figure 2: Free body diagram of the system

2.2 Kinematics and Dynamics

The state variables for the velocity are represented in the body reference frame but the state variables for position are in global frame. The transformation between the global and body coordinate frames is described as follows [20]:

$$\mathbf{x}^b = \mathbf{R}_G^b \mathbf{x}^G \quad (1)$$

$$\mathbf{x}^G = \mathbf{R}_b^G \mathbf{x}^G \quad (2)$$

$$\mathbf{R}_b^G = \begin{bmatrix} c_\psi c_\theta & s_\psi c_\theta & -s_\theta \\ c_\psi s_\phi s_\theta - c_\phi s_\psi & s_\phi s_\psi s_\theta + c_\phi c_\psi & c_\theta s_\phi \\ c_\phi c_\psi s_\theta + s_\phi s_\psi & c_\phi s_\psi s_\theta - c_\psi s_\phi & c_\phi c_\theta \end{bmatrix} \quad (3)$$

The relationship between the angular rates and the time derivatives of the *Euler* angles is:

$$\boldsymbol{\omega} = \begin{bmatrix} p \\ q \\ r \end{bmatrix} = \begin{bmatrix} 1 & 0 & -s_\theta \\ 0 & c_\phi & s_\phi c_\theta \\ 0 & -s_\phi & c_\phi c_\theta \end{bmatrix} \begin{bmatrix} \dot{\phi} \\ \dot{\theta} \\ \dot{\psi} \end{bmatrix} = \mathbf{S} \begin{bmatrix} \dot{\phi} \\ \dot{\theta} \\ \dot{\psi} \end{bmatrix} \quad (4)$$

If the *Euler* angles are assumed to be small (≈ 0), then the \mathbf{S} matrix becomes the identity matrix and the angular rates are roughly equal to the time derivative of the *Euler* angles. The thrust (T) of each motor being proportional to the product of the square of the angular velocity (ω) of the rotor shaft and a lift coefficient (K_T) such that:

$$T = K_T \omega^2 \quad (5)$$

The dynamics of the quadcopter can be derived using *Newton* second law. The linear equations of motion are defined in the global reference frame. The acceleration of the quadcopter in the global frame is equal to the sum of force of gravity, F_g , the thrust force of the motor, F_T^G , and linear friction force resulting in drag, F_d . This is given by:

$$m\ddot{X}^G = \begin{bmatrix} \dot{X}^G \\ \dot{Y}^G \\ \dot{Z}^G \end{bmatrix} = F_g - F_T^G - F_d = \begin{bmatrix} 0 \\ 0 \\ mg \end{bmatrix} + \begin{bmatrix} 0 \\ 0 \\ K_T \sum_{i=1}^4 \omega_i^2 \end{bmatrix} + \begin{bmatrix} K_{dx}\dot{X}^G \\ K_{dy}\dot{Y}^G \\ K_{dz}\dot{Z}^G \end{bmatrix} \quad (6)$$

Using the global frame for translational position, the transformation is expressed as:

$$\begin{bmatrix} \dot{X}^G \\ \dot{Y}^G \\ \dot{Z}^G \end{bmatrix} = \begin{bmatrix} c_\psi c_\theta & c_\psi s_\phi s_\theta - c_\phi s_\psi & c_\phi c_\psi s_\theta + s_\phi s_\psi \\ s_\psi c_\theta & s_\phi s_\psi s_\theta + c_\phi c_\psi & c_\phi s_\psi s_\theta - c_\psi s_\phi \\ -s_\theta & c_\theta s_\phi & c_\phi c_\theta \end{bmatrix} \begin{bmatrix} \dot{x}^b \\ \dot{y}^b \\ \dot{z}^b \end{bmatrix} \quad (7)$$

The translational equations of motion are defined with three positions, namely, forward (x), sideward (y) and altitude (z) as follows:

$$\begin{bmatrix} \ddot{x}^G \\ \ddot{y}^G \\ \ddot{z}^G \end{bmatrix} = \begin{bmatrix} \frac{1}{m} (-[c_\phi s_\theta c_\psi + s_\phi s_\psi] U_1 - k_{dx}\dot{X}^G) \\ \frac{1}{m} (-[c_\phi s_\theta s_\psi - s_\phi c_\psi] U_1 - k_{dy}\dot{Y}^G) \\ \frac{1}{m} (-[c_\phi c_\theta] U_1 - k_{dz}\dot{Z}^G) + g \end{bmatrix} \quad (8)$$

The rotational equations of motion are defined in the body reference frame. It comprises three terms, namely, the motors produce rolling, pitching and yawing torques, the gyroscopic effect resulting from the rigid body rotation and the cross product which describes the gyroscopic effect resulting from the propeller rotation coupled with the body rotation. This is represented by the following equation:

$$J_b \dot{\omega} = \tau_m - \tau_g - (\omega \times J_b \omega) \quad (9)$$

Meanwhile, the rotational equation of motion is expressed as:

$$\begin{bmatrix} \ddot{\phi} \\ \ddot{\theta} \\ \ddot{\psi} \end{bmatrix} = \begin{bmatrix} \frac{1}{J_x} [(J_y - J_z)qr - J_r q (\omega_1 - \omega_2 + \omega_3 - \omega_4) + U_2] \\ \frac{1}{J_y} [(J_z - J_x)pr - J_r q (\omega_1 - \omega_2 + \omega_3 - \omega_4) + U_3] \\ \frac{1}{J_z} [(J_x - J_y)pq + U_4] \end{bmatrix} \quad (10)$$

2.3 Quadcopter Physical Parameters

A set of standard of quadcopter physical parameters is adapted from [20]. The details of the parameters are shown in Table 1.

Table 1: Quadcopter physical and motor parameters

Description	Unit	Value
Quadcopter mass, m	kg	1.4
Distance from center of mass to each motor, l	m	0.56
Thickness of quadcopter's arms for drawing purposes, t	m	0.02
Radius of propeller, rad	m	0.1
Drag torque coefficient, K_D	kgm^2	1.3858e-6
Translational drag force coefficient, $[K_{Dx}, K_{Dy}, K_{Dz}]$	kg/s	[0.16481, 0.31892, 1.1e-6]
Moment of inertia about X axis, $[J_x, J_y, J_z]$	kgm^2	[0.05, 0.05, 0.24]

Gravity, g	m/s^2	9.81
Thrust force coefficient, K_T	kgm	1.3328e-5
Moment of inertia of the rotor, J_r (or J_p)	kgm^2	0.013
Motor speeds, lower & upper limits	rad/s	0 and 925

3.0 CONTROL

Two types of controllers were used in the quadcopter system. Firstly, it uses a modified PID control at the outermost loop control configuration unlike the traditional PID structure that presents a drawback [4, 20, 22]. Thus, a modified PID architecture as shown in Figure 3 based on Eq. (11) has been used and applied in this study. The PID control algorithm is written as:

$$u(t) = K_p e(t) + K_i \int_0^t e(t) dt + K_D \frac{e(t) - e(t-1)}{dt} \quad (11)$$

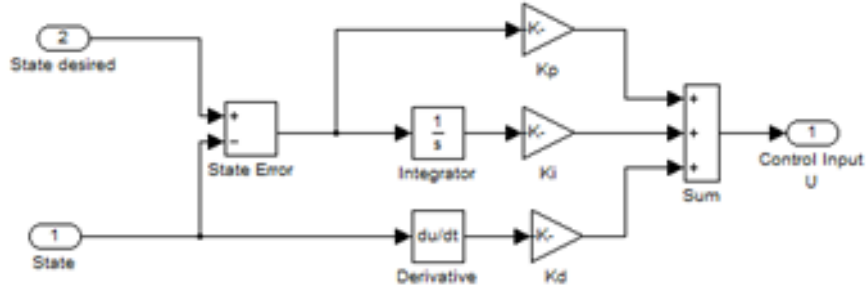


Figure 3: Modified PIDcontrol structure in MATLAB/Simulink

The overall PID control architecture of the quadcopter system can be seen in Figure 4.

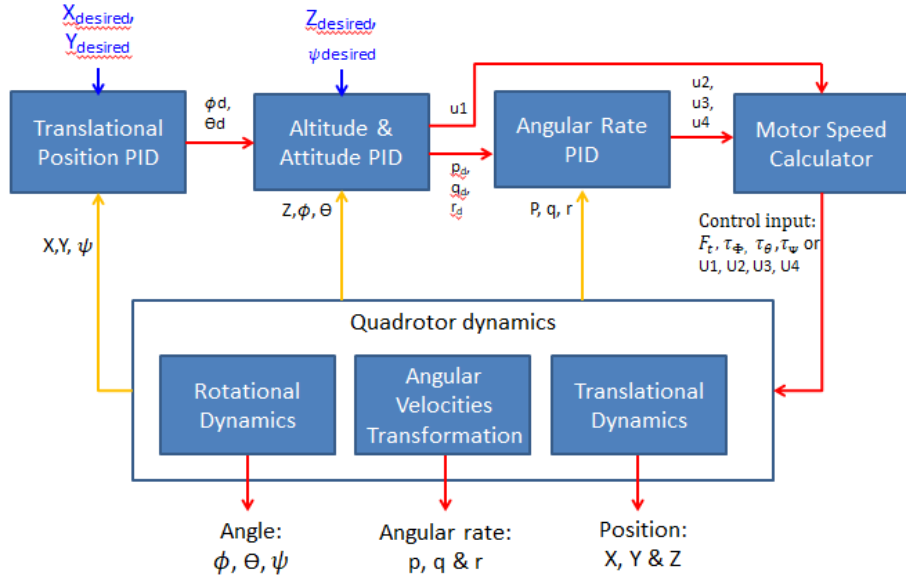


Figure 4: PID control structure for the quadcopter system

The AFC-based controller scheme as shown in Figure 5(a) has been implemented as an inner control loop which is simply added in series with the modified PID control scheme for the altitude and yaw control of the quadcopter. Figures 5(b) and 5(c) show the

AFC implementation in MATLAB/Simulink. Note that the AFC method primarily deals with the inertial (I') or mass (EM) parameters of the dynamic system to be multiplied with the measured acceleration (α' or a'). This resulting product is then subtracted from the measured torque or force. The summation of the two signals yields the estimated disturbance (Q') which is then passed through the inverse of the actuator function ($W(s)/K$) before being summed up with the outer PID control loop [14-17]. The typical AFC main equations are:

$$\text{For a rotational system: } Q' = T' - I' \alpha' \quad (12)$$

$$\text{For a translational system: } Q' = F' - EM a' \quad (13)$$

where the estimated disturbance, Q' is referring to the estimated torque for the rotational system and estimated force for the translational system. T' and F' are the measured torque and force, respectively.

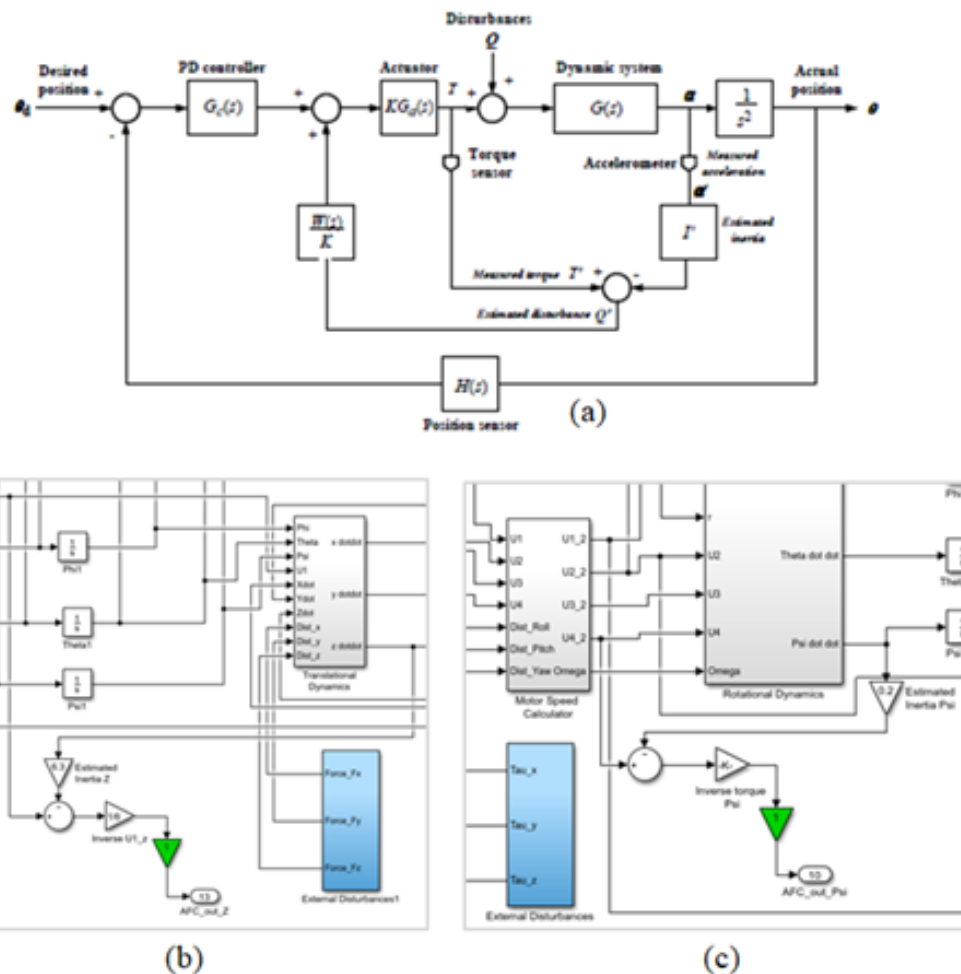


Figure 5: (a) General PID+AFC schematic (b) AFC section with estimated mass (EM) for altitude (Z-axis) control (c) AFC section with estimated inertia (I') for yaw control

The overall proposed PID+AFC control scheme can be seen in Figure 6.

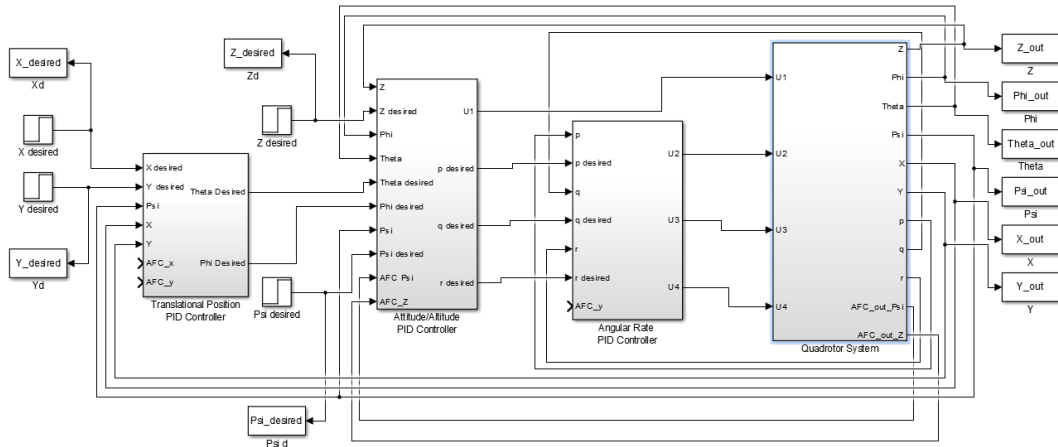


Figure 6: Simulink block diagram of the attitude/altitude control for the PID+AFC control scheme

4.0 SIMULATION

The MATLAB/Simulink computing platform was used to simulate and compare the control performances for both the PID only and PID+AFC approaches. The simulation include case studies related to two simple flight path commands with different types of disturbances. Flight path A is at hovering condition, $[X, Y, Z, \psi] = [0, 0, +1, 0]$ while flight path B is a simple 3D trajectory, $[X, Y, Z, \psi] = [+0.25, +0.25, +1, 0]$. A number of disturbances were added into the system. Note that no disturbance condition is applied in the rotational direction, i.e., $\tau_x = \tau_y = \tau_z = 0$. The response characteristics related to the maximum overshoot in amplitude and settling time were then analyzed. Before the AFC-based control mode is activated, all the gains of the PID controller, i.e., K_p , K_i and K_d must first be tuned appropriately based on the flight paths. The tuning uses a heuristic trial-and-error method and the resulting suitable gains were accordingly obtained. Once the PID gains were tuned, the AFC part is then activated and further tuning of the AFC parameters was initiated with reference to the acquisition of the estimated parameters/functions related to I , EM and $W(s)/K$.

5.0 RESULTS AND DISCUSSION

The overall simulation results are summarized and tabulated in Tables 2 and 3 according to the flight paths and types of disturbances. In most tests, both the PID and AFC-based schemes produce better results especially in altitude (Z) control, while there is a slight improvement for yaw control in the latter scheme (AFC+PID).

Table 2: Summary of the simulation results for flight paths A and B with no disturbances

Flight Path	Disturbance Type	Results
A	None	Both controllers show no significant differences in Z and Yaw responses except for a very little difference in the yaw position (ψ) for flight path A (refer to Figure 5)
B	None	

Table 3: Simulation results for flight paths A and B with disturbances

Type of Disturbance	Disturbance Direction & Magnitude	Flight Path A	Flight Path B
Constant force-i	$[X, Y, Z] = [3, 0, 1]$	Z steady state error is significantly improved (~25% reduction) with PID+AFC	PID+AFC has improved the Z steady state error (~25% reduction) and only a slight improvement in yaw control is observed especially in the magnitude of the overshoot
Constant force-ii	$[X, Y, Z] = [0, 1, 3]$	Z steady state error is significantly improved (~70% reduction) with PID+AFC	Significant improvement (~70%) in Z steady state error with PID+AFC and no difference in yaw control response for both controllers is observed
Impulsive force	$X = Y = 0$ Z: Amplitude, 3 N with period 10 s, width 10% and delay 1 s	With PID+AFC, the yaw control is slightly improved	No difference in Z and yaw responses
Payload mass	Added mass: 2 kg	With PID+AFC, the yaw control is slightly improved	A slight improvement in Z and yaw responses with PID+AFC in terms of the magnitude of overshoot
Vibration	$X & Y = 0$ (no vibration) $Z: 50\sin 100t$	With PID+AFC, the yaw control is slightly improved	No difference in both controllers for Z response and a slightly better performance in yaw control for PID+AFC is observed

The graphical results can be seen in Figures 7 and 8.

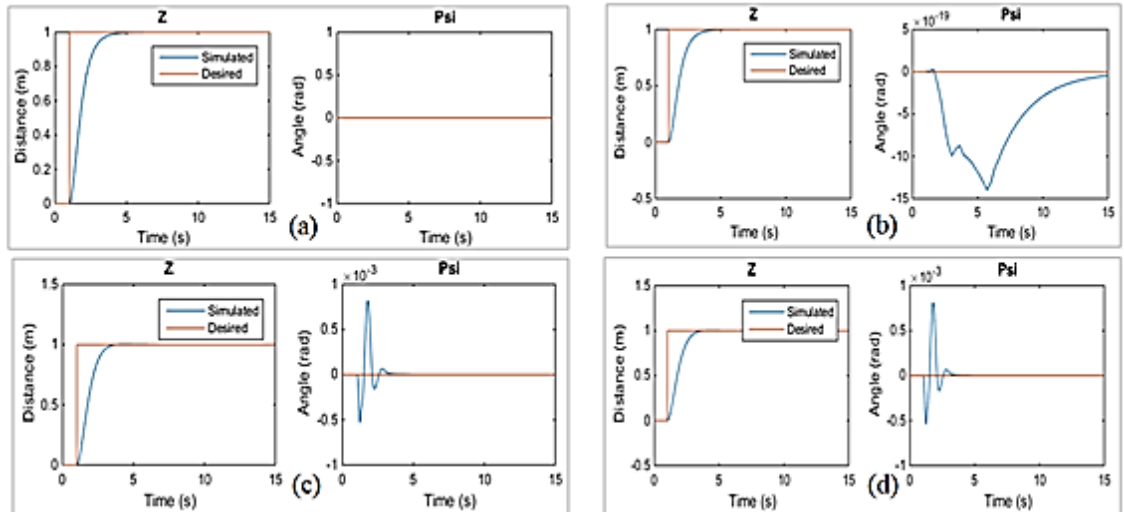


Figure 7: Z and yaw response results without disturbance for (a) flight path A with PID only (b) flight path A with PID+AFC (c) flight path B with PID only (d) flight path B with PID+AFC

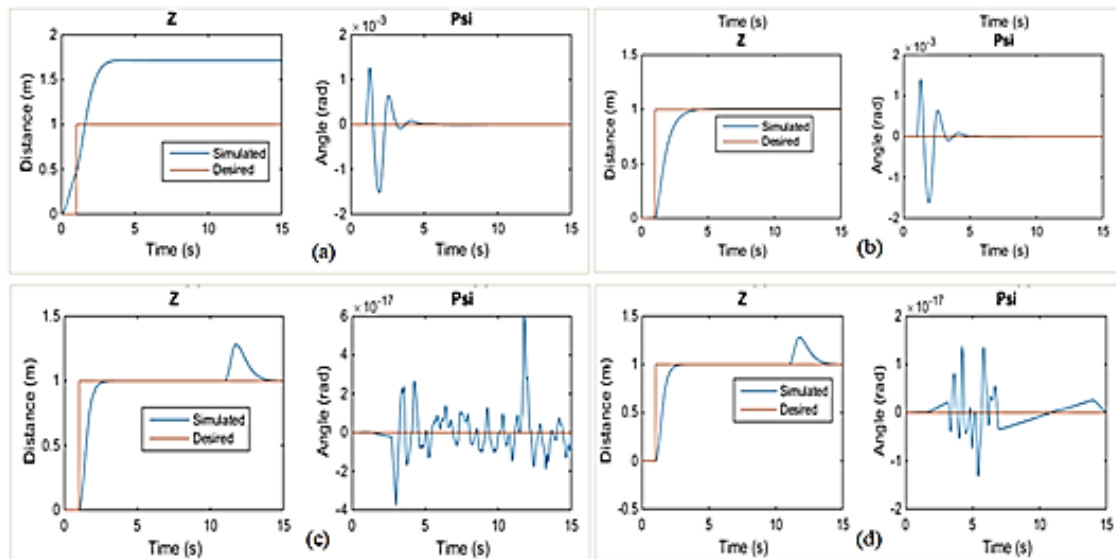


Figure 8: Z and yaw response results for (a) & (b) constant force-II for flight path B with PID only versus PID+AFC (c) & (d) impulse force for flight path A with PID only versus PID+AFC

6.0 CONCLUSION

The AFC-based method has been successfully implemented in altitude and yaw control of the quadcopter system. Both the PID and PID+AFC control approaches have been tested and compared with different flight paths and disturbances. The results show that the implementation of AFC has resulted in better control of the altitude with the presence of disturbances in the system. In other words, the PID+AFC scheme has significantly improved the altitude control where the steady state error can be reduced up to 70%, particularly in the presence of Z-axis disturbance. In most simulation case studies, for AFC-based scheme, the steady state condition of the altitude response can easily be controlled to reach the desired value with very minimal steady state error. Besides, the proposed scheme helps the system to react faster (shorter settling time) to maintain the quadcopter hovering state condition. However, only a slight improvement was seen in the yaw control even with the application of AFC. In future, the advantages of the AFC-based system can be further investigated in controlling the X and Y positions and the other attitude control related to roll and pitch movements. The actual PID+AFC scheme with actual disturbance applications can also be performed on a physical and real quadcopter in order to validate its performance based on the proposed method.

ACKNOWLEDGMENTS

The authors gratefully acknowledge FKM, UTM for providing the logistic and related facilities.

REFERENCES

1. Martinez V.M., 2007. *Modelling of The Flight Dynamics of A Quadrotor Helicopter*, Master of Science Thesis, Department of Aerospace Sciences, Cranfield University, UK.
2. Valavanis K.P., 2007. *Advances in Unmanned Aerial Vehicles: State of The Art and The Road to Autonomy*, Florida: Springer.
3. Bresciani T., 2008. *Modelling, Identification and Control of A Quadrotor Helicopter*, Master of Science Thesis, Department of Automatic Control, Lund University, Sweden.

4. Huang H., Hoffman G.M., Waslander S.L. and Tomlin C.J., 2009. Aerodynamics and Control of Autonomous Quadrotor Helicopters in Aggressive Maneuvering, IEEE International Conference on Robotics and Automation, Kobe, Japan.
5. Wang Y., Li P., Lan Z., Li B. and Li C., 2017. Quadrotor Aircraft Design Based on The K60 Controller, *J. Eng. Sci. Technol. Rev.*, 10(6): 21–30.
6. Praveen V. and Pillai A.S., 2016. Modeling and Simulation of Quadcopter Using PID Controller, *International Journal of Control Theory and Applications*, 9(15): 7151–7158.
7. Smirnova M.A. and Smirnov M.N., 2017. Dynamic Modeling and Hybrid Control Design with Image Tracking for A Quadrotor UAV, *International Journal of Applied Engineering Research*, 12(15): 5073-5077.
8. Alkamachi A. and Ercelebi E., 2018. H_∞ Control of An Overactuated Tilt Rotors Quadcopter., *J. Cent. South Univ*, 25(3): 586-599.
9. Fan Y., Cao, Y. and Zhao Y., 2017. Design of the Non-linear Controller for A Quadrotor Trajectory Tracking, *Proceedings of the 29th Chinese Control And Decision Conference (CCDC)*, Chongqing, China, July 26-28.
10. Fan Y., Cao Y. and Zhao Y., 2017. Sliding Mode Control for Non-linear Trajectory Tracking of A Quadrotor, *Proceedings of the 36th Chinese Control Conference*, Dalian, China, July 26-28.
11. Shekhar R.C., Kearney M. and Shames I., 2015. Robust Model Predictive Control of Unmanned Aerial Vehicles Using Waysets, *J. Guid. Control Dyn.*, 38(10): 1898–1907.
12. Tiep D.K. and Ryoo, Y.-J., 2017. An Autonomous Control of Fuzzy-PD Controller for Quadcopter, *Int. J. Fuzzy Log. Intell. Syst.*, 17(2): 107–113.
13. Mailah M., 1998. *Intelligent Active Force Control of A Rigid Robot Arm Using Neural Network and Iterative Learning Algorithms*, PhD Thesis, University of Dundee, UK.
14. Mailah M., Hewit J.R. and Meeran S., 1996. Active Force Control Applied to A Rigid Robot Arm, *Jurnal Mekanikal*, 2(2): 52-68.
15. Pitowarno E., Mailah M. and Jamaluddin H., 2002. Knowledge-Based Trajectory Error Pattern Method Applied to An Active Force Control Scheme, *International Journal of Engineering and Technology*, 2(1): 1-15.
16. Noshadi A., Mailah M. and Zolfagharian A., 2012. Intelligent Active Force Control of A 3-RRR Parallel Manipulator Incorporating Fuzzy Resolved Acceleration Control, *Applied Mathematical Modelling*, 36(6), 2370-2383.
17. Priyandoko G., Mailah M. and Jamaluddin H., 2009. Vehicle Active Suspension System Using Skyhook Adaptive Neuro Active Force Control, *Mechanical Systems and Signal Processing*, 23(3): 855-868.
18. Nor N.S.M. and Mailah M., 2011. Vibration Suppression of Hard Disk Drive Mechanism Using Intelligent Active Force Control, *4th International Conference on Mechatronics (ICOM)*, Kuala Lumpur, Malaysia.
19. Varatharajoo R., Choo T.W. and Mailah M., 2011. Two Degree of Freedom Spacecraft Attitude Controller, *Advances in Space Research*, 47(4): 685-689.
20. Wil Selby, A Record of My Tech Research and Travel Adventures, ArduCopter, <https://www.wilselby.com/research/arducopter/> [Accessed: 15 Sep 2017].
21. Mian A.A. and Wang D.-b., 2008. Dynamic Modeling and Non-linear Control Strategy for An Underactuated Quad Rotor Rotorcraft, *Jounal of Zhejiang University - SCIENCE A*, 9(4): 539-545.
22. de Oliveira M.D.L.C., 2011. *Modeling, Identification and Control of A Quadrotor Aircraft*, Master Thesis, Department of Control Engineering, Faculty of Electrical Engineering, Czech Technical University, Prague.